Swelling of Diffusive Fluid Threads in Microchannels

Thomas Cubaud*
Department of Mechanical Engineering, Stony Brook University, Stony Brook, New York 11794, USA

(Received 7 May 2020; revised 29 July 2020; accepted 25 September 2020; published 23 October 2020)

The dynamics of viscous fluid threads concurrently flowing with miscible solvents is experimentally investigated in square microchannels. Diffusive fluid threads are found to significantly swell at low flow velocities due to large specific interfacial area and hydrodynamic lubrication. An approach based on bounded function analysis of confined thread diameter is developed to model diffusive behavior of viscosity-differing fluids at the small scale. This work shows the determination of a critical flow rate associated with each fluid pair and the use of dynamic similarity to calculate diffusion coefficients between oils and organic solvents. The thread divergence is estimated based on the growth of diffusion layers and related to diffusion-induced buckling instabilities of viscous threads in parallel flows.

DOI: 10.1103/PhysRevLett.125.174502

Fluid threads comprise a broad class of slender viscous structures that are commonly encountered in industrial processes, including fiber synthesis [1] and electrospray [2], and often occur in natural situations, such as during the coiling of a liquid rope [3–5], or during the capillary breakup of confined jets [6–8]. While gravity and inertia play an important role at the large scale, the behavior of two liquids flowing at the small scale is closely related to the magnitude of their viscosity coefficients η_1 and η_2, as well as interfacial tension γ_{12} for immiscible fluids or diffusion coefficient D_{12} for miscible fluid pairs. Diffusive fluid displacement in porouslike media have shown the emergence of distinct miscible liquid structures, such viscous fingers and spikes, depending on the Péclet number Pe [9,10]. Microfluidic systems provide precise control over flow geometry and flow rates of injection, and the use of hydrodynamic focusing sections are practical to investigate mass transfer phenomena between fluids having similar viscosities $\eta_1 \sim \eta_2$ [11–13]. In the case of large viscosity contrasts $\eta_1 \gg \eta_2$, lubricated threads of fluid $L1$ can readily form in a low-viscosity phase $L2$ using a simple channel intersection [14]. Miscible core-annular flows display complex dynamics [15,16], including diffusive and inertial instabilities [17], as well as viscous buckling instabilities [18–20], which are of particular interest for the generation of crimped and helical microfibers [21–23].

Lubricated microfluidic threads also have large specific interfacial area compared to two-fluid layered flows and this property offers advantages for the development of continuous hydrodynamic methods for enhancing micromixing of viscosity-differing fluids [24] as well as for examining mass transfer mechanisms with complex fluids [25]. Determination of diffusion coefficients D_{12} between fully miscible fluids in the context of large viscosity contrasts $\chi = \eta_1/\eta_2$, however, requires the use of advanced experimental techniques [26–28]. Steady-state measurements and theoretical modeling of D_{12} at large χ are also challenging due to the spatial evolution of fluid viscosity and concentration gradients in the diffusive region [29]. In addition, numerous fluids of industrial interest, such as alcohols and polymers, are only partially miscible and form nonideal, conjugate solutions depending on their solubility [30]. Therefore, generic microfluidic methods are needed for the rapid characterization of D_{12} between fully and partially miscible fluids made of chemically different species with various molecular affinities, such as between nonpolar viscous oils and polar organic solvents.

Here, the thread-forming ability of high-viscosity fluids is used to examine the relationship between convective and diffusive transport between high-molecular weight solutes and low-molecular weight solvents in confined microsystems. A method based on novel phenomenological and mathematical understanding of diffusive fluid threads in microchannels is developed to determine diffusion coefficients between fully and partially miscible fluids. The growth of diffusion layers around the thread is also shown to induce viscous buckling instabilities in straight microchannels.

Microfluidic platforms are made of glass and silicon where square microchannels of height $h = 250$ μm form an orthogonal focusing section. The thick fluid $L1$ is injected at volume flow rate Q_1 into the central channel and the thin fluid $L2$ is symmetrically introduced in the side channels at Q_2 using syringe pumps [Fig. 1(a)]. The device is placed on top of an inverted microscope and illuminated with a fiber light for high-speed imaging. Fluids are made of conventional silicone oils and low-molecular weight alcohols.

Stable threads correspond to steady core-annular flows with a central stream of width ε_0. In the absence of interfacial tension and neglecting diffusion, solution of Stokes equation [15] in a circular tube of diameter h

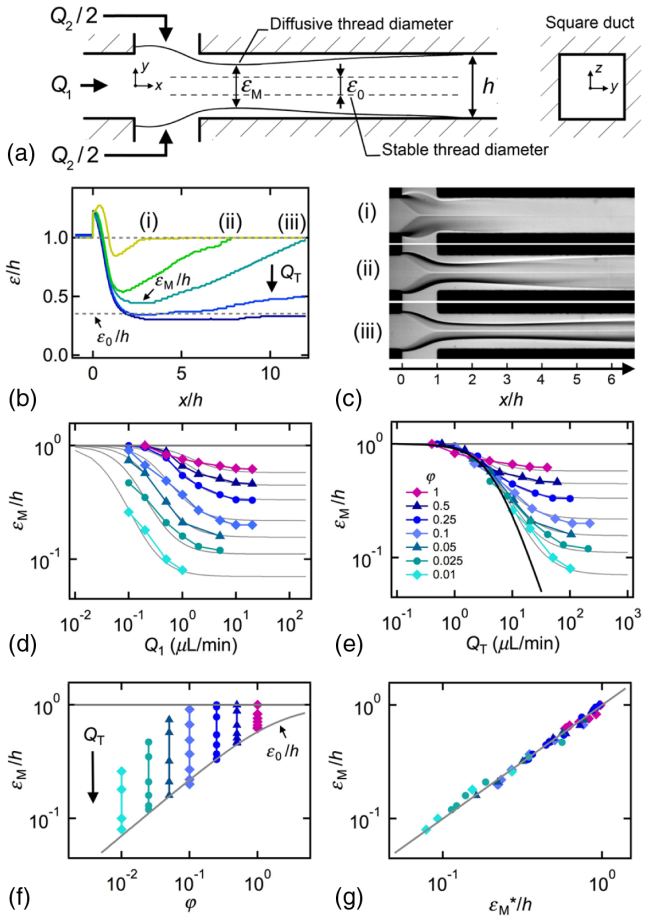

FIG. 1. (a) Schematic of diffusive threads. (b) Spatial evolution of thread diameter ε/h for $\varphi = 0.25$, (i) $Q_T = 5$, (ii) 10, and (iii) 25 μL/min with 100-cS silicone oil and isopropanol. (c) Experimental micrographs corresponding to (b). (d)–(f) Evolution of ε_M/h at various φ as a function of Q_1, Q_T, and φ (see text for details). (f) Comparison of ε_M/h and ε_M^*/h calculated based on Eq. (2). Solid line: $\varepsilon_M/h = \varepsilon_M^*/h$.

indicates that for large viscosity contrast $\chi \gg 1$, the expression for the core diameter ε_0 reduces to

$$\frac{\varepsilon_0}{h} = \left(\frac{\varphi}{2+\varphi}\right)^{1/2}, \tag{1}$$

which yields the scaling $\varepsilon_0/h \sim (\varphi/2)^{1/2}$ for small flow rate ratio $\varphi = Q_1/Q_2$. Equation (1) provides a useful basis to examine the behavior of diffusive fluid threads in square microchannels.

At low flow rates, miscible threads are seen to significantly swell and a minimum diameter ε_M is found in excess of ε_0 as shown on Fig. 1(a). Since the stable diameter ε_0 depends on φ, experiments are conducted by fixing the relative flow rate $\varphi = Q_1/Q_2$ while varying the absolute flow rate $Q_T = Q_1 + Q_2$. Figure 1(b) shows the spatial evolution of the normalized central stream width ε/h for $\varphi = 0.25$ when $L1$ is made 100-cS silicone oil and $L2$ consists of isopropanol [Fig. 1(c)]. As ε/h grows at the junction, a minimal value ε_M is measured in the outlet channel before widening further downstream. Data show that ε_M tends to ε_0 at large Q_T while ε_M tends to h at small flow rates. The quantity ε_M is practical as it provides a single measurement to characterize the role of diffusion on thread morphology. Therefore, we examine the influence of Q_1 and Q_T on the variation of ε_M for fixed values of φ. On the one hand, plotting ε_M as a function of Q_1 [Fig. 1(d)] ungroups iso-φ curves, which appear distinct and bounded with varying slopes. On the other hand, displaying ε_M as a function of Q_T [Fig. 1(e)] regroups iso-φ data onto a master curve at low Q_T and shows the progressive separation of each curve from the trend as ε_M tends to ε_0 at large Q_T. The asymptotic behavior of ε_M for large Q_T is evident when represented as a function of φ in conjunction with Eq. (1) on Fig. 1(f).

As experimental data show that, for a given fluid pair at fixed φ, ε_M depends on Q_T and ranges between 1 and ε_0, we briefly discuss the use of bounded functions to model the evolution of ε_M. A simple expression of S-shaped function corresponds to $f(x) = 1/(a + x^b)$ with $a > 0$. In the case where $a = 1$, symmetry properties indicate that $f(x) = f^C(x^{-1})$, where the complementary function $f^C = 1\text{-}f$. Therefore, a bounded function can also be described using a complementary function of a reciprocal variable. In general, as $f = a^{-1}$ when $x^b \to 0$, the sign of variable b indicates whether f tends to a^{-1} when $x \to 0$ for $b > 0$ or when $x \to \infty$ for $b < 0$. The magnitude of b corresponds to the steepness of the curve between the bounded values of 0 and a^{-1} for f or between 1 and $1\text{-}a^{-1}$ for f^C. Therefore, given the boundary conditions of ε_M/h, a complementary bounded function of the form

$$\frac{\varepsilon_M^*}{h} = 1 - \frac{1}{\dfrac{1}{1-\varepsilon_0/h} + \left(\dfrac{Q_T}{Q_C}\right)^{-1.5}} \tag{2}$$

is proposed to model thread behavior. The steepness value of $b = -1.5$ is found to best fit the overall shape of curves for all fluid pairs and is therefore postulated as constant. By contrast, the value Q_C corresponds to the offset of Q_T and is specific to each fluid pair. The evolution of ε_M/h along iso-φ curves is calculated using Eqs. (1) and (2), and is displayed as a thin line for each φ curve on Fig. 1(e). In practice, determination of the fitting parameter Q_C is made along iso-φ curves in the (ε_M/h, Q_1) parameter space displayed on Fig. 1(d) using $Q_T = Q_1(1 + \varphi^{-1})$ as individual curves are distinguishable and do not overlap with one another. Finally, observed values of ε_M/h and predicted values of ε_M^*/h are found to closely match as shown in Fig. 1(g). In conclusion, the method of analyzing bounded functions along iso-φ curves of diffusive threads permits the determination of a single kinematic quantity Q_C associated with each fluid pair.

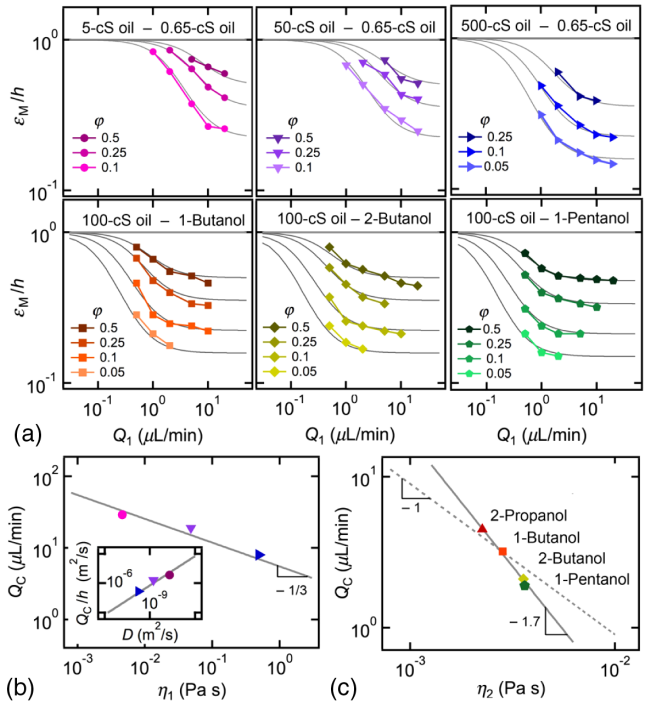

FIG. 2. (a) Evolution of ε_M/h along φ curves as a function of Q_1 for various fluid pairs as indicated with $L1$ and $L2$. (b) Critical flow rate Q_C versus inner viscosity η_1 for oil fluid pairs. Solid line: $Q_C = 5.5\eta_1^{-1/3}$. Inset: Q_C/h vs diffusion coefficient D. Solid line: $Q_C/h = \mathrm{Pe}_C D$ with $\mathrm{Pe}_C = 850$. (c) Critical flow rate Q_C versus outer viscosity η_2 oil and alcohol fluid pairs. Solid line: $Q_C = 1.4 \times 10^{-4}\eta_2^{-1.7}$; dashed line: $Q_C = 9 \times 10^{-3}\eta_2^{-1}$.

To better understand the relationship between Q_C and the intermolecular coefficient of diffusion D_{12}, we apply the iso-φ technique to fully miscible silicone oil fluid pairs and we examine a few soluble silicone oil and alcohol fluid pairs as shown in Fig. 2(a). In each case, a single critical flow rate Q_C is found to closely fit data for each fluid pair. The diffusion coefficient D_{12} between a solute made of large molecules having hydrodynamic radius R_1 and a solvent of low-molecular weight having viscosity η_2 can be inferred using the Stokes-Einstein equation, $D_{12} = kT/(6\pi\eta_2 R_1)$, where k is the Boltzmann constant and T is the temperature [31]. Hydrodynamic modeling of D_{12} is useful for the case of fully miscible fluids having similar chemical affinity, such as silicone oils of various molecular weights, where the hydrodynamic radius is assumed to scale as $R_1 \sim \eta_1^{0.34}$ based on the manufacturer's data sheet (Gelest) [32]. In this situation, the product $D\eta_2\eta_1^{0.34}$ is expected to remain constant at room temperature and can be estimated from tabulated values [26] to determine D_{12} for a given oil pair.

Here, the solvent viscosity of oil pairs is kept constant at $\eta_2 = 0.49$ mPa s (0.65 cS) and η_1 is varied according to 4.6 (5 cS), 48 (50 cS), and 487 mPa s (500 cS). The measured values of Q_C are plotted as a function of η_1 in Fig. 2(b) and data are well fitted with $Q_C \sim \eta_1^{-1/3}$, which in turn suggests $Q_C \sim D_{12}$. Since the Péclet number $\mathrm{Pe} = Q/(hD_{12})$ quantifies the relative influence of convection and diffusion, we compare Q_C/h to the values of D_{12} estimated using the hydrodynamic approach and find

$$\frac{Q_C}{h} = \mathrm{Pe}_C D_{12}, \tag{3}$$

where the critical $\mathrm{Pe}_C = 850$ for fully miscible fluids [Fig. 2(b), inset]. The same method of determining Q_C is applied to the partially miscible oil and alcohol cases, where $\eta_1 = 97$ mPa s (100-cS oil) is fixed and $\eta_2 = 2.25$ (isopropanol), 2.83 (1-butanol), 3.57 (2-butanol), and 3.62 mPa s (1-pentanol). Over the limited range of solvent viscosity, data suggest $Q_C \sim \eta_2^{-1.7}$, which is in significant deviation from Stokes-Einstein prediction, as one would expect $Q_C \sim \eta_2^{-1}$ [Fig. 2(c)]. Departure from theory is not unexpected as silicone oils and low-molecular alcohols have different chemical affinity and the configuration of a polymer in solution, such as its hydrodynamic radius R_1, is known to strongly depend on the interaction with the solvent [30,33]. In particular, alcohols can be considered as "poor" solvents for silicone oils since, for instance, we observe that a 100-cS silicone oil can be partially dissolved in butanol and pentanol but not in ethanol nor hexanol. Dynamic similarity, however, can be used to estimate the effective D_{12} for partially miscible oil and alcohol fluid pairs using Eq. (3), which yields the following estimates: $D \approx 3.5 \times 10^{-10}$ (isopropanol), 2.5×10^{-10} (1-butanol), 1.6×10^{-10}, (2-butanol), and 1.5×10^{-10} (1-pentanol) m^2/s with an evaluated uncertainty in the range of $\Delta D \approx 10^{-11}$ m^2/s based on the calculation of the critical flow rate with $\Delta Q_C \approx 0.2$ μL/ min. Hence, microfluidic determination of Q_C provides useful information about the initial flow interaction between chemically different fluids, which is characterized using an effective diffusion coefficient by analogy with fully miscible fluids.

Another aspect of the swelling of diffusive threads resides in the development of a diffusion layer δ downstream from the location of ε_M. As can be seen in Fig. 1(b), the spatial evolution of ε appears quasilinear beside its bounded nature. To quantify thread swelling, we measure the location L_F where $\varepsilon \approx h$ and the datum L_M where $\varepsilon \approx \varepsilon_M$ as a function of the reduced flow rate Q_T/Q_C as indicated in Fig. 3(a). Both quantities depend on Q_T according to $L_F/h = 5.3(Q_T/Q_C)$ and $L_M/h = 1.5(Q_T/Q_C)^{1/2}$ [Fig. 3(b)]. Scaling relationships for L_M and L_F are used to estimate the thread divergence $\boldsymbol{\nabla}\cdot\boldsymbol{\varepsilon}$, where $\boldsymbol{\varepsilon} = \varepsilon\boldsymbol{i}$ and $\boldsymbol{i}$ is the vector unit in the x direction, in the straight channel due to diffusion according to $\boldsymbol{\nabla}\cdot\boldsymbol{\varepsilon} = d\varepsilon/dx = (h - \varepsilon_M)/(L_F - L_M)$. Since $d\varepsilon/dx$ depends on ε_M, which in turns depends on φ, we use the method of iso-φ curves with a few selected cases in Fig. 3(c). For $Q_T < Q_C$, $d\varepsilon/dx$ remains nearly constant while the divergence becomes inversely proportional to Q_T for $Q_T > Q_C$. This behavior is expected as the exponent

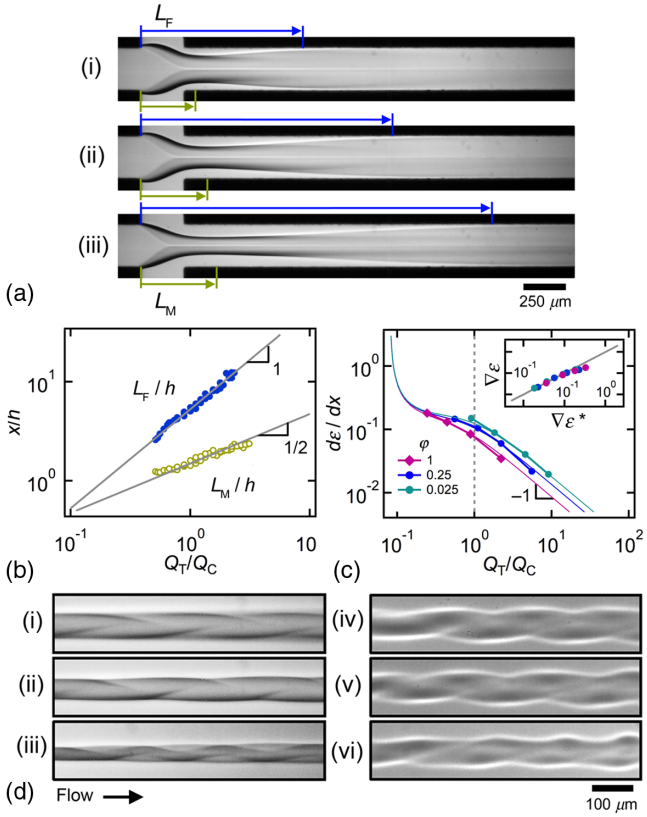

FIG. 3. (a) Examples of measurement of L_F and L_M from micrographs. Fluid pair: 100-cS oil and isopropanol. Flow rates in $\mu L/\text{min}$ (i) $(Q_1, Q_2) = (1, 2)$, (ii) (1, 4), and (iii) (1, 6). (b) Evolution of L_M and L_F as a function of Q_T/Q_C. Solid lines: $L_M/h = 1.5(Q_T/Q_C)^{1/2}$ and $L_F/h = 5.3(Q_T/Q_C)$. (c) Evolution of $\nabla \cdot \varepsilon$ with Q_T/Q_C for various φ. Inset: Comparison of $\nabla \cdot \varepsilon$ and $\nabla \cdot \varepsilon^*$ calculated from Eq. (4). Solid line: $\nabla \cdot \varepsilon = \nabla \cdot \varepsilon^*$. (d) Micrographs showing internal buckling. Fluid pairs: from (i) to (iii) 100-cS oil and isopropanol and from (iv) to (vi) 0.65-cS and 500-cS oils. (i) $(Q_1, Q_2,) = (0.5, 17)$, (ii) (0.5, 25), (iii) (0.5, 40), (iv) (1,60), (v) (1, 70), and (vi) (1, 90).

associated to the evolution of L_F becomes dominant for large Q_T, which leads to the approximation

$$\vec{\nabla} \cdot \vec{\varepsilon}^* = a\left(1 - \frac{\varepsilon_0}{h}\right)\left(\frac{Q_T}{Q_C}\right)^{-1}, \tag{4}$$

where $a = 1/5.3$. As can be seen in Fig. 3(c), inset, good agreement is found between data and Eq. (4). The thread divergence can also be expressed using Eq. (3) as $\boldsymbol{\nabla} \cdot \boldsymbol{\varepsilon}^* = b(\varepsilon_0^C/h)\text{Pe}^{-1}$, where the thread complementary diameter $\varepsilon_0^C = h - \varepsilon_0$ and $b \approx 160$. Thus, our analysis suggests the diffusion layer scales as $\delta \sim x/\text{Pe}$. This result compares with Taylor dispersions where $\delta \sim (x/\text{Pe})^{1/3}$ in the upstream region and $\delta \sim (x/\text{Pe})^{1/2}$ in the downstream region [34,35] taking into consideration the confined nature of δ and the use of scaling laws with varying exponents. Such "ultradiffusive" behavior of lubricated threads is interpreted as resulting from their large interfacial area and location at the centerline of parabolic stokes flows as opposed to stratified flows where diffusion primarily occurs near the solid walls.

Finally, the growth of the diffusion layer has implications on the structural stability of small threads. Previous analysis highlights the complex radial composition of miscible fluid threads having a highly viscous core of diameter ε_0 unsheathed within a swelled layer of diameter ε_M forming near the fluid contactor. In turn, the swelled thread is enclosed within a diffusive layer δ that further develops downstream. Thus, the highly viscous core experiences an overall deceleration as a result of swelling behavior of its envelope, which hints at the development of a dynamic compressive force along the thread axis to conserve momentum based on rudimentary control volume analysis. Experimental evidence of diffusion-induced buckling of viscous threads is displayed on Fig. 3(d) where threads are seen to coil within their diffusive envelope for small ε/h at large Q_T/Q_C. Complementary theoretical and numerical work taking into account the development of transient stresses in the diffusive region would help further clarify internal buckling of diffusive fluid threads in parallel microflows.

Overall, the viscous regime of lubricated threads provides a useful reference to characterize mass diffusion phenomena between viscosity-differing fluids. Here, a thread-based method is developed in conjunction with bounded function analysis of iso-φ curves to identify a single kinematic quantity Q_C associated with each fluid pair. In turn, information about Q_C is employed to calculate an effective diffusion coefficient D_{12} using similitude arguments. This approach of determining Q_C does not require any particular assumption about D_{12} and can be applied to a variety of fully and partially miscible fluid pairs having large viscosity contrasts. Techniques based on microfluidic viscous threads are promising for probing the role of fluid properties on diffusion as well as for characterizing diffusion-limited reactions with high-viscosity fluids. Future work could also examine the flow behavior of partially miscible fluids systems in relation with spontaneous emulsification phenomena to advance both practical understanding and modeling of viscous fluid interactions in confined microsystems.

This material is based upon work supported by the National Science Foundation under Grant No. CBET-1150389.

*Author to whom correspondence should be addressed.
thomas.cubaud@stonybrook.edu

[1] O. du Roure, A. Lindner, E. N. Nazockdast, and M. J. Shelley, Dynamics of flexible fibers in viscous flows and fluids, Annu. Rev. Fluid Mech. **51**, 539 (2019).
[2] A. Barrero and I. G. Loscertales, Micro- and nanoparticles via capillary flows, Annu. Rev. Fluid Mech. **39**, 89 (2007).

[3] M. Maleki, M. Habibi, R. Golestanian, N. M. Ribe, and D. Bonn, Liquid Rope Coiling on a Solid Surface, Phys. Rev. Lett. **93**, 214502 (2004).
[4] P.-T. Brun, B. Audoly, N. M. Ribe, T. S. Eaves, and J. R. Lister, Liquid Ropes: A Geometrical Model for Thin Viscous Jet Instabilities, Phys. Rev. Lett. **114**, 174501 (2015).
[5] N. M. Ribe, Liquid rope coiling: A synoptic view, J. Fluid Mech. **812**, R2 (2017).
[6] P. Guillot, A. Colin, A. S. Utada, and A. Ajdari, Stability of a Jet in Confined Pressure-Driven Biphasic Flow at Low Reynolds Numbers, Phys. Rev. Lett. **99**, 104502 (2007).
[7] A. S. Utada, A. Fernandez-Nieves, J. M. Gordillo, and D. A. Weitz, Absolute Instability of a Liquid Jet in a Coflowing Stream, Phys. Rev. Lett. **100**, 014502 (2008).
[8] J. Molenaar, G. N. van Heugten, and C. J. M. van Rijn, Viscous liquid threads with inner fluid flow inside microchannels, ACS Omega **4**, 9800 (2019).
[9] T. Suekane, J. Ono, A. Hyodo, and Y. Nagatsu, Three-dimensional viscous fingering of miscible fluids in porous media, Phys. Rev. Fluids **2**, 103902 (2017).
[10] E. Lajeunesse, J. Martin, N. Rakotomalala, D. Salin, and Y. C. Yortsos, Miscible displacement in a Hele-Shaw cell at high rates, J. Fluid Mech. **398**, 299 (1999).
[11] J. B. Knight, A. Vishwanath, J. P. Brody, and R. H. Austin, Hydrodynamic Focusing on a Silicon Chip: Mixing Nanoliters in Microseconds, Phys. Rev. Lett. **80**, 3863 (1998).
[12] R. F. Ismagilov, A. D. Stroock, P. J. A. Kenis, G. M. Whitesides, and H. A. Stone, Experimental and theoretical scaling laws for transverse diffusion broadening in two-phase laminar flows in microchannels, Appl. Phys. Lett. **76**, 2376 (2000).
[13] J. Goulpeau, B. Lonetti, D. Trouchet, A. Ajdari, and P. Tabeling, Building up longitudinal concentration gradients in shallow microchannels, Lab Chip **7**, 1154 (2007).
[14] T. Cubaud and T. G. Mason, Folding of Viscous Threads in Diverging Microchannels, Phys. Rev. Lett. **96**, 114501 (2006).
[15] D. D. Joseph and Y. Y. Renardy, Fundamentals of Two-Fluid Dynamics, *Part II: Lubricated Transport, Drops and Miscible Liquids* (Springer-Verlag, New York, 1993).
[16] B. Selvam, S. Merk, R. Govindarajan, and E. Meiburg, Stability of miscible core-annular flows with viscosity stratification, J. Fluid Mech. **592**, 23 (2007).
[17] T. Cubaud and S. Notaro, Regimes of miscible fluid thread formation in microfluidic focusing sections, Phys. Fluids **26**, 122005 (2014).
[18] T. Cubaud and T. G. Mason, Swirling of Viscous Fluid Threads in Microchannels, Phys. Rev. Lett. **98**, 264501 (2007).
[19] S. Gosh, G. Das, K. Prasanta, and K. Das, Liquid buckling in a practical situation, Eur. Phys. Lett. **115**, 44004 (2016).
[20] B. Xu, J. Chergui, S. Shin, and D. Juric, Three-dimensional simulations of viscous folding in diverging microchannels, Microfluid. Nanofluid. **20**, 140 (2016).
[21] J. K. Nunes, H. Constantin, and H. A. Stone, Microfluidic tailoring of the two-dimensional morphology of crimped microfibers, Soft Matter **9**, 4227 (2013).
[22] A. Duboin, R. Middleton, F. Malloggi, F. Monti, and P. Tabeling, Cusps, spouts and microfiber synthesis with microfluidics, Soft Mater. **9**, 3041 (2013).
[23] Y. Yu, F. Fu, L. Shang, Y. Cheng, Z. Gu, and Y. Zhao, Bioinspired helical microfibers from microfluidics, Adv. Mater. **29**, 1605765 (2017).
[24] T. Cubaud, Segmented flows of viscous threads in microchannels, Phys. Rev. Fluids **4**, 084201 (2019).
[25] K. Gowda, C. Brouzet, T. Lefranc, L. D. Söderberg, and F. Lundell, Effective interfacial tension in flow-focusing of colloidal dispersions: 3-D numerical simulations and experiments, J. Fluid Mech. **876**, 1052 (2019).
[26] N. Rashidnia, R. Balasubramaniam, J. Kuang, P. Petitjeans, and T. Maxworthy, Measurement of diffusion coefficient of miscible fluids using both interferometry and Wiener's method, Int. J. Thermophys. **22**, 547 (2001).
[27] A. Bouchaudy, C. Loussert, and J.-B. Salmon, Steady microfluidic measurements of mutual diffusion coefficients of liquid binary mixtures, AIChE J. **64**, 358 (2018).
[28] J. Dambrine, B. Géraud, and J.-B. Salmon, Interdiffusion of liquids of different viscosities in a microchannel, New J. Phys. **11**, 075015 (2009).
[29] J. Crank, *The Mathematics of Diffusion* (Oxford Univeristy Press Inc., New York, 1975).
[30] G. W. Castellan, *Physical Chemistry* (Addison-Wesley Publishing Company, Reading, Massachusetts, 1983).
[31] R. B. Bird, W. E. Stewart, and E. N. Lightfoot, *Transport Phenomena* (John Wiley & Sons, Inc., New York, 2002).
[32] T. Cubaud and T. G. Mason, Formation of miscible fluid microstructures by hydrodynamic focusing in plane geometries, Phys. Rev. E **78**, 056308 (2008).
[33] J. Israelachvili, *Intermolecular and Surface Forces* (Academic Press, Amsterdam, 1991).
[34] J. Jiménez, The growth of a mixing layer in a laminar channel, J. Fluid Mech. **535**, 245 (2005).
[35] J.-B. Salmon and A. Ajdari, Transverse transport of solutes between co-flowing pressure-driven streams for microfluidic studies of diffusion/reaction processes, J. Appl. Phys. **101**, 074902 (2007).